Supporting Information

Rational synthesis of 3D coral-like $ZnCo_2O_4$ nanoclusters with abundant oxygen vacancies for high-performance supercapacitors

Yanlei Bi, [a] Huiqing Fan, [a*] Chuansen Hu, [a] Ru Wang, [a] Lujie Niu, [a] Guangwu Wen,[b] and Luchang Qin [c]

[a] School of Chemistry and Chemical Engineering, Shandong University of Technology, Zibo 255000, China

[b] School of Materials Science and Engineering, Shandong University of Technology, Zibo 255000, China

[c] Department of Physics and Astronomy, University of North Carolina at Chapel Hill, Chapel Hill, NC 27599-3255, USA

Table S1 Weight variations of Ni foam after different treatments during experiment.

	Ni foam pure	**Ni foam** after hydrothermal reaction	**Ni foam** after calcination	**Ni foam** after $NaBH_4$ reduction
Mass(mg)	178.81	181.80	181.22	180.97

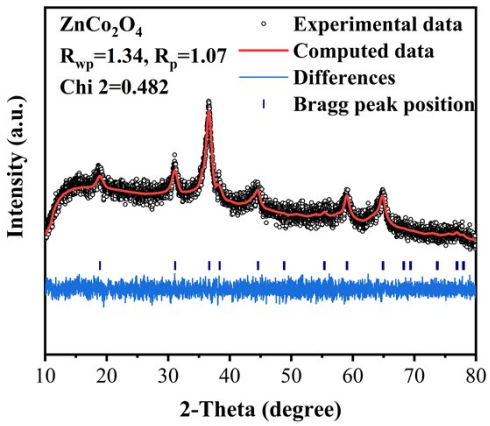

Fig.S1. X-ray diffraction pattern and the Rietveld refinement results of $ZnCo_2O_4$

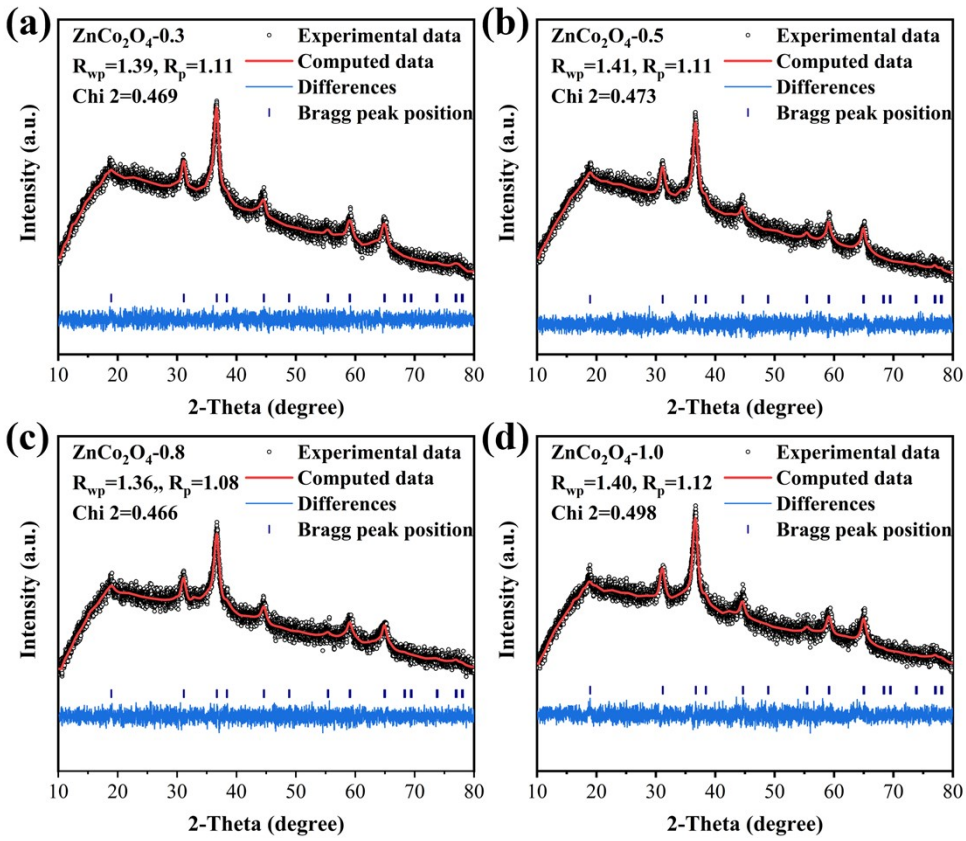

Fig. S2. X-ray diffraction pattern and the Rietveld refinement result of (a) $ZnCo_2O_4$-0.3, (b) $ZnCo_2O_4$-0.5, (c) $ZnCo_2O_4$-0.8, and (d) $ZnCo_2O_4$-1.0.

Table S2 The refined lattice parameters of $ZnCo_2O_4$ and OV-$ZnCo_2O_4$.

Sample	**Zn:Co:O**	**R_p**	**R_{wp}**	**R_{exp}**	**Chi 2**	**Relative crystallinity**
$ZnCo_2O_4$	1:2:3.90	1.07	1.34	1.93	0.482	57.24 %
$ZnCo_2O_4$-0.3	1:2:3.81	1.11	1.39	2.03	0.469	52.61 %
$ZnCo_2O_4$-0.5	1:2:3.66	1.11	1.41	2.04	0.473	50.70 %
$ZnCo_2O_4$-0.8	1:2:3.52	1.08	1.36	2.00	0.466	49.59 %
$ZnCo_2O_4$-1.0	1:2:3.36	1.12	1.40	1.98	0.498	44.86 %

The relative crystallinity of $ZnCo_2O_4$ and OV-$ZnCo_2O_4$ was calculated by the following formula[1, 2]:

$$\varepsilon = \frac{I_c}{I_c + I_a} \times 100\% \quad (1)$$

where ε is the relative crystallinity, I_c is the integral strength of crystallization peaks, and I_a is the integral strength of amorphous peaks.

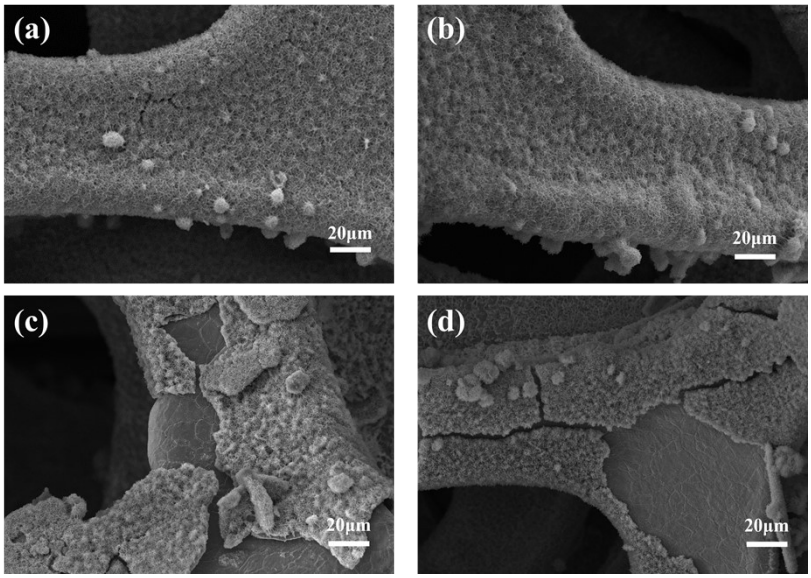

Fig. S3. (a-d) SEM images of $ZnCo_2O_4$-0.3, $ZnCo_2O_4$-0.5, $ZnCo_2O_4$-0.8 and $ZnCo_2O_4$-1.0.

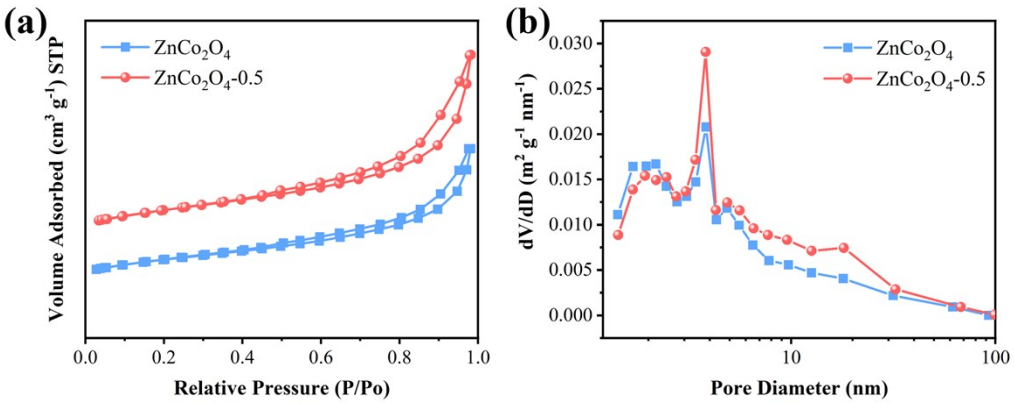

Fig. S4. (a) N_2 adsorption-desorption isotherms, and (b) pore size distribution of pristine $ZnCo_2O_4$ and $ZnCo_2O_4$-0.5 nanoclusters.

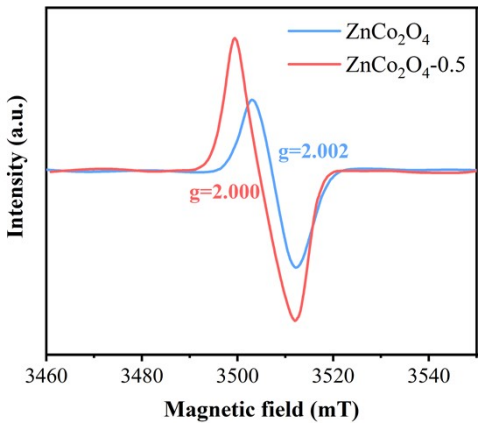

Fig. S5. EPR spectra of pristine $ZnCo_2O_4$ and $ZnCo_2O_4$-0.5 nanoclusters.

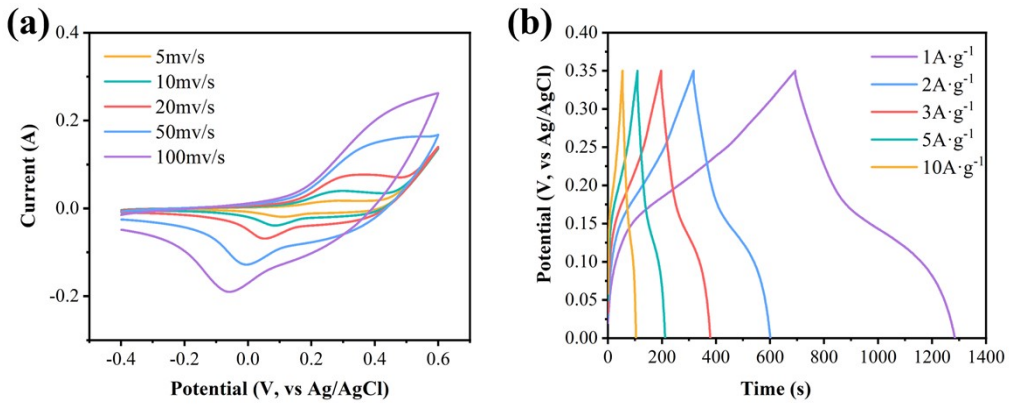

Fig. S6. (a) CV curves at different scan rates of pristine $ZnCo_2O_4$, (b) GCD curves at different current densities of pristine $ZnCo_2O_4$.

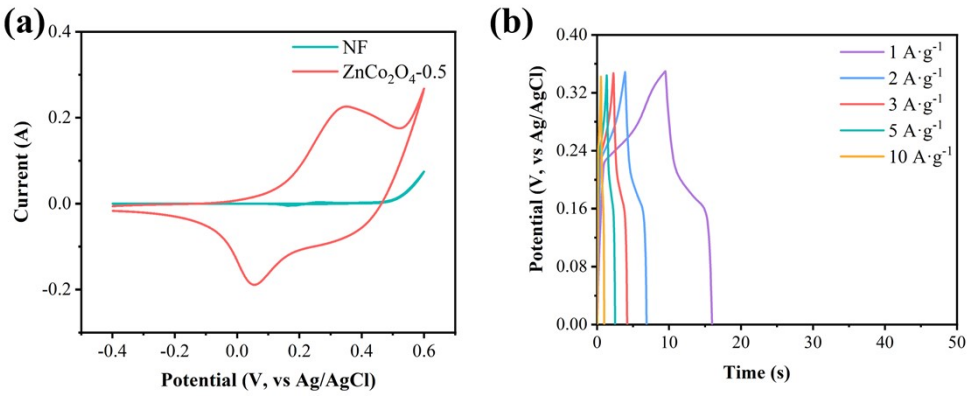

Fig. S7. (a) CV curves at different scan rates of $ZnCo_2O_4$-0.5 and Ni foam, (b) GCD curves at different current densities of Ni foam.

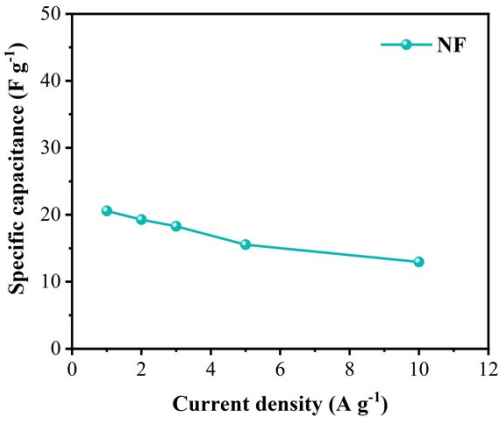

Fig. S8. Specific capacitances of Ni foam at different current densities.

Table S3 Comparison of the electrochemical properties between the coral-like $ZnCo_2O_4$ nanoclusters and recent results reported in literature.

Materials	Electrolyte	Voltage window	Specific capacitance	Cycling Stability	Ref.
S-doped $ZnCo_2O_4$ microspindles	3 M KOH	0-0.4 V	522 F g^{-1} at 0.5 A g^{-1}	78% after 5,000 cycles at 3 A g^{-1}	[3]
graphene nanoplatelets/ $ZnCo_2O_4$ microspheres	6 M KOH	0-0.45 V	960 F g^{-1} at 1 A g^{-1}	78.9% after 2,000 cycles at 5 A g^{-1}	[4]
Marigold-Like $ZnCo_2O_4$	1 M KOH	0-0.5 V	1167 F g^{-1} at 1 A g^{-1}	81.3% after 10,000 cycles at 30 mA cm^{-2}	[5]
$ZnCo_2O_4$@rGO nanocomposite	3 M KOH	0-0.4 V	1830 F g^{-1} at 3 A g^{-1}	90% after 10,000 cycles at 15 mA cm^{-2}	[6]
N-doped $ZnCo_2O_4$@rGO nanocomposite	2 M KOH	0-0.6 V	950 F g^{-1} at 1 A g^{-1}	89.6% after 5,000 cycles at 1 A g^{-1}	[7]
NiCoMn-S@ $ZnCo_2O_4$ nanowires	3 M KOH	0-0.5 V	1671 C g^{-1} at 1.1 A g^{-1}	76.48% after 3,000 cycles at 50 mA cm^{-2}	[8]
$ZnCo_2O_4$@ $NiCo_2O_4$ nanocomposite	6 M KOH	0-0.5 V	1728 F g^{-1} at 1 A g^{-1}	97.8% after 2,000 cycles at 10 A g^{-1}	[9]
Coral-like $ZnCo_2O_4$ nanoclusters	6 M KOH	0-0.35 V	2685.7 F g^{-1} at 1 A g^{-1}	72.59% after 10,000 cycles at 3 A g^{-1}	This work

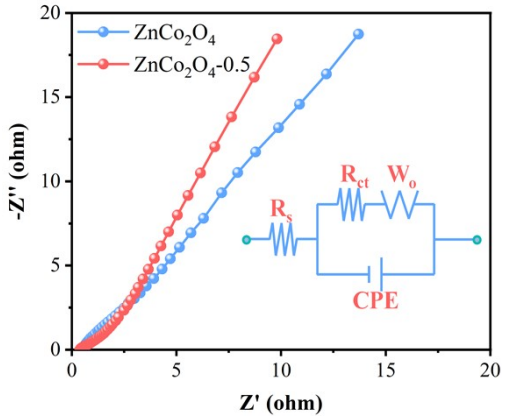

Fig. S9. EIS curves of pristine $ZnCo_2O_4$ and $ZnCo_2O_4$-0.5 nanoclusters, with the inset showing the corresponding equivalent circuit.

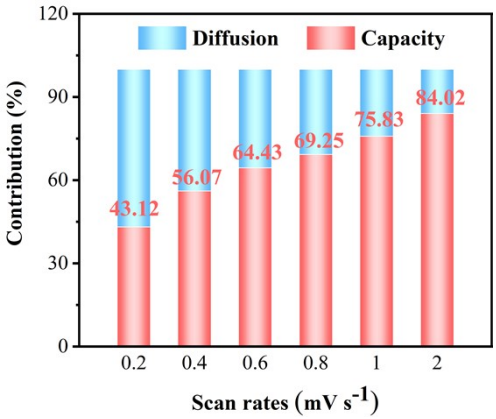

Fig. S10. Contributions of capacitance-controlled (red region) and diffusion-controlled (blue region) processes at different scan rates of $ZnCo_2O_4$ nanoclusters

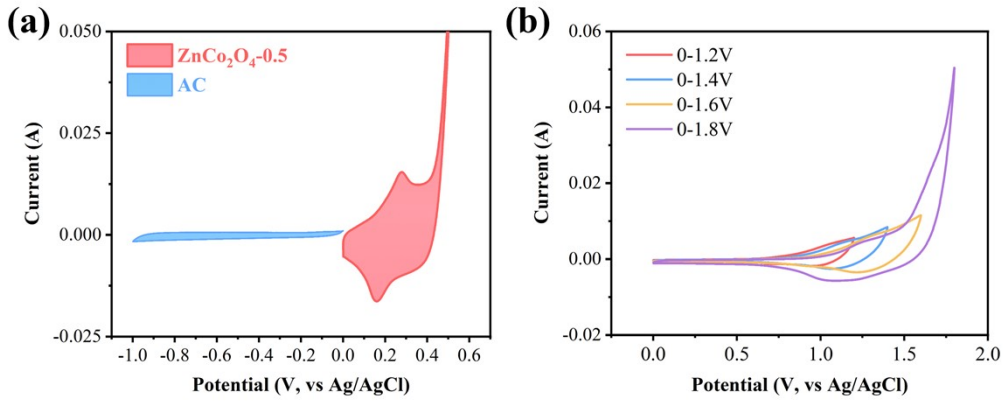

Fig. S11. (a) CV curves of $ZnCo_2O_4$-0.5 and AC, (b) CV curves of $ZnCo_2O_4$-0.5 nanoclusters//AC ASC device with varying voltage windows.

References

[1] B. Zhang, L. Gao, H. Bai, Y. Li, B. Jia, X. Zhou, A. Li and L. Li, *J. Alloys Compd.*, 2023, 934, 167979.

[2] N. Ashraf, M. Aadil, S. Zulfiqar, H. Sabeeh, M.A. Khan, I. Shakir, P.O. Agboola and M.F. Warsi, *ChemistrySelect*, 2020, 5, 8129-8136.

[3] Y. Yang, C. Yang, K. Tao, Q. Ma and L. Han, *Vacuum*, 2020, 181, 109740.

[4] B. Huang, Q. Tang, C. Liang, N. Liu and Y. Wang, *Mater. Lett.*, 2021, 298, 130022.

[5] M.M. Faras, S.S. Patil, P.S. Patil and A.P. Torane, *J. Energy Storage*, 2023, 74, 109490.

[6] B. Naresh, C. Kuchi, S.K. Kummara, O.R. Ankinapalli and P.S. Reddy, *Synth. Met.*, 2023, 293, 117283.

[7] G. Vignesh, R. Ranjithkumar, P. Devendran, N. Nallamuthu, S. Sudhahar and M. Krishna Kumar, *Mater. Sci. Eng., B*, 2023, 290, 116328.

[8] H. Wang, W. Cai, L. He, M. Zhu and Y. Wang, *J. Alloys Compd.*, 2021, 870, 159347.

[9] Z. Wu, X. Yang, H. Gao, H. Shen, H. Wu, X. Xia, X. Wu, W. Lei, J. Yang and Q. Hao, *J. Alloys Compd.*, 2022, 891, 162053.